Modeling, Analysis and Simulation of 3D Elastohydrodynamic Revolute Joints in Multibody Systems

P. Flores

Abstract In this work, a methodology for dynamic analysis of rigid-flexible multibody systems with elastohydrodynamic (EHD) lubricated joints is presented. The EHD lubricated cylindrical joint is formulated by the Natural Coordinate Formulation (NCF) and the twenty-node hexahedral element of Absolute Nodal Coordinate Formulation (ANCF), being the lubricant pressure determined through the resolution of the Reynolds' equation employing the finite difference method. The outcomes are validated with those obtained by using the commercial software ADINA. It is demonstrated that the bearing flexibility plays a significant role in the system responses, extends the lubricant distribution space and reduces the lubricant pressure.

Keywords Revolute joints · Elastohydrodynamic lubrication · Multibody dynamics

1 Introduction

A mechanical system usually consists of two major kinds of components, bodies and joints [6]. The bodies can be modeled as rigid or flexible elements, while the joints are represented by a set of kinematic constraints. The functionality of a mechanical joint relies upon the relative motion allowed between the connected components. This fact implies the existence of a clearance between the mating parts, and thus joint surfaces can contact each other or may be separated with a lubricant. It is of paramount importance to quantify the effects of both clearance joints and bodies flexibility on the global system response in order to define the minimum level of suitable tolerances that allow systems to achieve required performances.

P. Flores (✉)
University of Minho, Guimares, Portugal
e-mail: pflores@dem.uminho.pt

M. Ceccarelli and E.E. Hernández Martinez (eds.), *Multibody Mechatronic Systems*,
Mechanisms and Machine Science 25, DOI 10.1007/978-3-319-09858-6_19

In practice, lubricant is often utilized in mechanical joints to avoid the body-to-body (typically metal-to-metal) contact. This measure can reduce the level of impact and vibrations, and extends the joints lifetime. It is quite important to develop appropriate computational models that can account for the lubricant action in mechanical joints in the context of multibody system dynamics. For this purpose, two kinds of approaches can be found in the scientific domain of tribology, namely the hydrodynamic (HD) theory and the elastohydrodynamic (EHD) formulation. According to the HD theory, in the presence of dynamics of journal bearings, the hydrodynamic forces, which include both squeeze and wedge effects, generated by the lubricant fluid, oppose the journal motion. The hydrodynamic forces can be obtained by integrating the pressure distribution evaluated with the aid of Reynolds' equation established for the dynamic regime. Liu et al. [5] and Attia et al. [1] are among the very few authors who performed the EHD analysis for lubricated high-speed rotor-bearing systems by using the Fluid-Structure Interaction (FSI) analysis. These studies clearly demonstrated that the bearing deformations affect the pressure field in the clearance and increase the minimal film thickness. However, these works were performed only for isolated journal bearing systems.

2 Rigid-Flexible Multibody Formulation

In the present study, the flexible parts such as the flexible bearing and beams are modeled by using the finite elements of Absolute Nodal Coordinate Formulation (ANCF). In the ANCF, the location and deformation of a material point in a finite element are defined in a global coordinate system, such that no coordinate transformation is required and the mass matrix remains constant while the centrifugal and Coriolis forces in the finally derived dynamic equations vanish. The rigid bodies such as the journal in the cylindrical joint are described by NCF proposed by Jalón and Bayo [3]. It is known that NCF can also lead to a constant mass matrix for the rigid multibody system. The method that combines NCF describing the rigid bodies and ANCF describing the flexible bodies was named as the Absolute Coordinate Based (ACB) by Tian et al. [10], and has been widely adopted so that the mass matrix for the whole rigid-flexible system keeps constant and the system constraint conditions can be easily simplified. This approach is quite convenient from the computational point of view.

For a spatial rigid cylinder shown in Fig. 1, its motion can be defined, according to NCF, through two basic points and two unit vectors. Thus, the 12 global generalized coordinates of the rigid cylinder can be expressed as

$$\mathbf{q} = [\mathbf{r}_i^T, \mathbf{r}_j^T, \mathbf{u}^T, \mathbf{v}^T]^T \tag{1}$$

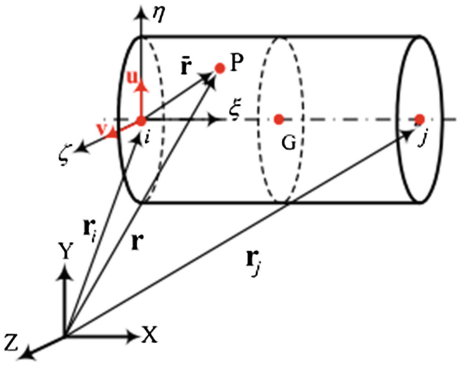

Fig. 1 Lubricant pressure distribution

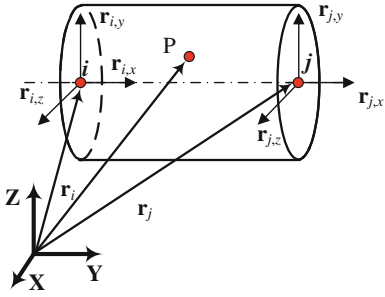

Fig. 2 Elastic deformation of bearing surface

where $\mathbf{r}_i$ and $\mathbf{r}_j$ are the position vectors of the basic points i and j, respectively. The vectors $\mathbf{u}$ and $\mathbf{v}$ are assumed to be unit and perpendicular vectors. The global position of an arbitrary point in the body can be written in the following form

$$\mathbf{r} = \mathbf{Cq} \tag{2}$$

where matrix $\mathbf{C}$ is determined by the local position ($\bar{\mathbf{r}}$) of point P defined in the body coordinate frame ξ-η-ζ, as Fig. 1 illustrates.

Different types of finite elements of ANCF have been proposed for modeling flexible parts undergoing both large overall motion and large deformation. In present study, the original two-node 3D beam element of ANCF developed by Shabana and Yakoub [8] is used to model flexible beams. There are a total of 24 nodal coordinates for each element, as depicted in Fig. 2.

3 EHD Model of Lubricated Cylindrical

In a broad sense, a suitable lubrication system can prevent body-to-body contact, reduce wear and, consequently, extend the service life of mechanical joints. With the intent to develop the EHD model of lubricated cylindrical joint with flexible bearing,

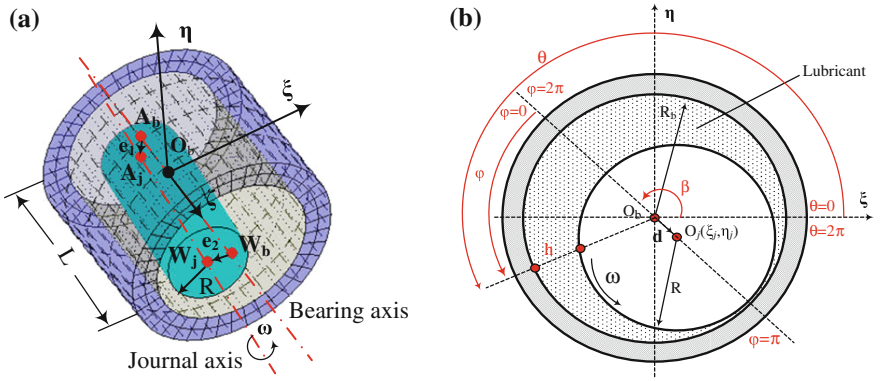

Fig. 3 **a** Generic configuration. **b** Arbitrary *cross section* along local axis ζ

the Reynolds' equations must be established. Figure 3a shows a generic configuration of a typical lubricated cylindrical joint, in which the journal misalignment is also represented. In the present study, the lubricated cylindrical joint is described by the ACB method. The center of mass of the bearing is denoted by point O_b and the journal bearing length by L. The local coordinate system is denoted by $\xi - \eta - \zeta$. In Fig. 3a, A_b and W_b are the bearing centers at end faces, while $A_j(\xi_1, \eta_1, -L/2)$ and $W_j(\xi_2, \eta_2, L/2)$ denote the journal centers at end faces. Figure 3b shows an arbitrary journal bearing cross section along the joint local axis ζ.

From Fig. 3a, when the journal misalignment is taken into account, the coordinates of an arbitrary journal cross section center O_j can be determined by the points $A_j(\xi_1, \eta_1, -L/2)$ and $W_j(\xi_2, \eta_2, L/2)$ from the following interpolation relations

$$\begin{aligned} \xi_j &= \xi_2 + \frac{(\xi_2 - \xi_1)(\zeta - L/2)}{L} \\ \eta_j &= \eta_2 + \frac{(\eta_2 - \eta_1)(\zeta - L/2)}{L} \end{aligned} \tag{3}$$

With regard to Fig. 3b, the general form of the isothermal Reynolds' equation can be expressed as [7]

$$\frac{\partial}{\partial\varphi}\left(h^3\frac{\partial p}{\partial\varphi}\right) + R^2\frac{\partial}{\partial\zeta}\left(h^3\frac{\partial p}{\partial\zeta}\right) = 6\mu R^2\omega\frac{\partial h}{\partial\varphi} + 12R^2\mu\frac{\partial h}{\partial t} \tag{4}$$

where p denotes the lubricant pressure, μ is the dynamic lubricant viscosity and R is the journal radius. The lubricant film thickness can be calculated by

$$h = c + d\cos\varphi = c + d\cos(\theta - \beta) = c - \xi_j\cos\theta - \eta_j\sin\theta \tag{5}$$

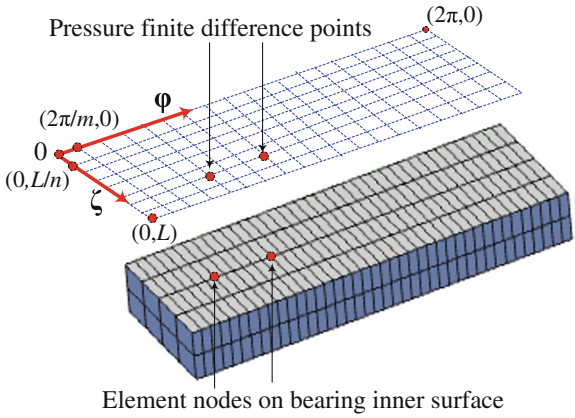

Fig. 4 EHD model of a lubricated cylindrical joint

in which c is the radial clearance, d represents the journal bearing eccentricity, θ is the angular coordinate and the variable β yields

$$\beta = \tan^{-1}\left(\frac{\eta_j}{\xi_j}\right) \tag{6}$$

When the elastic deformation of bearing is considered, the lubricant film thickness can be expressed in the following form

$$h = c - \xi_j \cos\theta - \eta_j \sin\theta + \delta \tag{7}$$

where δ denotes the elastic deformation of bearing.

As it is shown in Fig. 4, a lubricated cylindrical joint can be unfolded along with circumferential direction (ϕ). Then, the lubricant pressure field can be evaluated by imposing Eq. (8) to each calculation grid point of a finite-difference method [4]. The equal interval grid is adopted at both circumferential and axial directions. In Fig. 4, m and n represent the total number of finite difference points along circumferential direction (ϕ) and axial direction (ζ), respectively.

In order to evaluate the lubricant pressure, the Reynolds' equation (4) can be rewritten in the following form

$$h^3 \frac{\partial^2 p}{\partial \varphi^2} + 3h^2 \frac{\partial h}{\partial \varphi}\frac{\partial p}{\partial \varphi} + R^2 h^3 \frac{\partial^2 p}{\partial \zeta^2} + 3R^2 h^2 \frac{\partial h}{\partial \zeta}\frac{\partial p}{\partial \zeta} = 6\mu R^2 \omega \frac{\partial h}{\partial \varphi} + 12R^2 \mu \frac{\partial h}{\partial t} \tag{8}$$

According to the finite-difference method [7], the finite difference equation of the pressure can be expressed by

$$\left[\frac{-3h_{i,j}^2}{4(\Delta\varphi)^2}\left(h_{i+1,j}-h_{i-1,j}\right)+\frac{h_{i,j}^3}{(\Delta\varphi)^2}\right]p_{i-1,j}+\left[\frac{-3R^2h_{i,j}^2}{4(\Delta\zeta)^2}\left(h_{i,j+1}-h_{i,j-1}\right)+\frac{R^2h_{i,j}^3}{(\Delta\zeta)^2}\right]p_{i,j-1}$$
$$+\left[\frac{-2h_{i,j}^3}{(\Delta\varphi)^2}-\frac{2R^2h_{i,j}^3}{(\Delta\zeta)^2}\right]p_{i,j}+\left[\frac{3R^2h_{i,j}^2}{4(\Delta\zeta)^2}\left(h_{i,j+1}-h_{i,j-1}\right)+\frac{R^2h_{i,j}^3}{(\Delta\zeta)^2}\right]p_{i,j+1}$$
$$+\left[\frac{-3h_{i,j}^2}{4(\Delta\varphi)^2}\left(h_{i+1,j}-h_{i-1,j}\right)+\frac{h_{i,j}^3}{(\Delta\varphi)^2}\right]p_{i+1,j}=3\mu R^2\omega\frac{h_{i+1,j}-h_{i-1,j}}{\Delta\varphi}+12R^2\mu\left(\frac{\partial h_{i,j}}{\partial t}\right) \tag{9}$$

where $p_{i,j}$ is the pressure at the finite difference point (i, j), $i = 1, 2, ..., m$ and $j = 1, 2, ..., n$. Here, the pressure boundary conditions are $p(\varphi,0) = p(\varphi, L) = 0$, $p(\varphi_1, 0) = p(\varphi_2, L)$ and $p(\varphi_1, \zeta) = p(\varphi_2, \zeta)$, with φ_1 and φ_2 being the angles of the start and end point of a hydrodynamic film. In this work, the finite difference Eq. (9) is solved by using Successive Over Relaxation (SOR) method, that is

$$p_{i,j}=p_{i,j}+\lambda\left(a_0-a_1p_{i-1,j}-a_2p_{i,j-1}-a_3p_{i,j+1}-a_4p_{i+1,j}\right)/a_5 \tag{10}$$

where the six coefficients yield

$$a_0=3\eta R^2\omega\frac{h_{i+1,j}-h_{i-1,j}}{\Delta\varphi}+12R^2\mu\left(\frac{\partial h_{i,j}}{\partial t}\right)$$
$$a_1=\frac{-3h_{i,j}^2}{4(\Delta\varphi)^2}\left(h_{i+1,j}-h_{i-1,j}\right)+\frac{h_{i,j}^3}{(\Delta\varphi)^2}$$
$$a_2=\frac{-3R^2h_{i,j}^2}{4(\Delta\zeta)^2}\left(h_{i,j+1}-h_{i,j-1}\right)+\frac{R^2h_{i,j}^3}{(\Delta\zeta)^2}$$
$$a_3=\frac{3R^2h_{i,j}^2}{4(\Delta\zeta)^2}\left(h_{i,j+1}-h_{i,j-1}\right)+\frac{R^2h_{i,j}^3}{(\Delta\zeta)^2}$$
$$a_4=\frac{-3h_{i,j}^2}{4(\Delta\varphi)^2}\left(h_{i+1,j}-h_{i-1,j}\right)+\frac{h_{i,j}^3}{(\Delta\varphi)^2}$$
$$a_5=\frac{-2h_{i,j}^3}{(\Delta\varphi)^2}-\frac{2R^2h_{i,j}^3}{(\Delta\zeta)^2}$$

This procedure is performed until the pressure convergent criterion for the $(k + 1)$ step is reached, that is

$$\frac{\sum_{i=1}^{m}\sum_{j=1}^{n}\left|p_{i,j}^{(k+1)}-p_{i,j}^{(k)}\right|}{\sum_{i=1}^{m}\sum_{j=1}^{n}p_{i,j}^{(k+1)}}\leq tol \tag{11}$$

where *tol* is a specified convergence tolerance. It must be stated that in the present work the tolerance considered was equal to 10^{-5}. The pressure field is calculated only over the positive part by setting the pressure in the remaining portion equal to zero. This boundary condition, associated with the pressure field, corresponds to Gümbel's boundary conditions or half Sommerfeld's conditions [7]. Once the lubricant pressures at the finite difference points are obtained, they are transformed into the corresponding generalized nodal forces for analyzing the elastic deformation of flexible bearing. Finally, the elastic deformation δ of flexible bearing described by Eq. (7) can be evaluated according to the classic finite element method.

4 Results and Discussion

The purpose of this section is to demonstrate that the twenty-node hexahedral element of ANCF can be applicable to a flexible hollow cylinder subjected to distributed forces as shown in Fig. 5. The distributed forces acting on the cylinder are assumed to be a linear function in time, defined as $F = 1000t$ N/m. The inner radius, length and thickness of the cylinder are equal to 0.225, 0.2, and 0.05 m, respectively. The Young's modulus of the bearing material is equal to 1×10^6 Pa.

Figure 6 shows the influence of mesh size on the displacement of point B in *Z*-direction and indicates that 4(axial direction) × 2(radial direction) × 40(circumferential direction) elements are enough to obtain the converged results.

In order to validate the obtained numerical results, the same model is also analyzed by using the commercial software ADINA [2]. The 3D 20-node brick solid element is used to mesh the model. From Fig. 7, the von Mises stresses at points A and B obtained by the numerical method are well agreement with those obtained by ADINA. Figure 8 shows the dynamic configurations and the von Mises stress contours of the hollow cylinder at different instants. Figure 9 shows the von Mises stress contour of the hollow cylinder obtained by using ADINA at the instant time $t = 1.00$ s. Also, after a careful analysis of the results represented in Figs. 8 and 9 leads to the assertion that the twenty-node hexahedral finite element of ANCF exhibits a very close response to the case of ADINA simulations. For this example

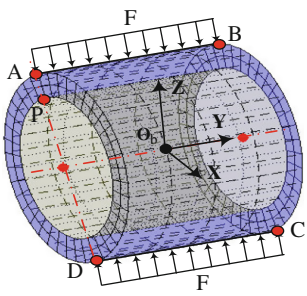

Fig. 5 A flexible *hollow cylinder* under uniform distribution forces

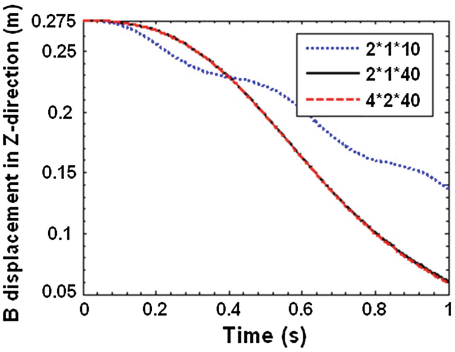

Fig. 6 Influence of the model mesh size on the displacement of point *B* in *Z-direction*

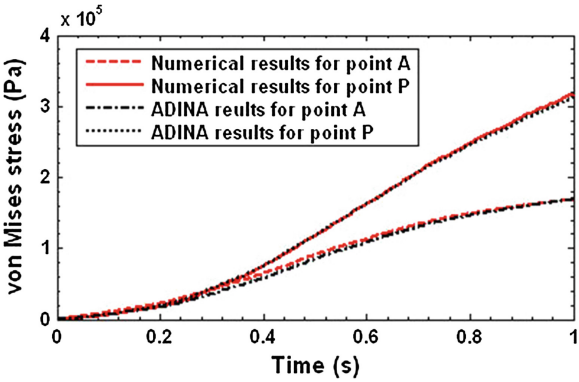

Fig. 7 Comparison of the von Mises stresses at *points A* and *P* numerical results versus ADINA results

the integration step is set to be 1e-3s, the cost computation time for the ADINA software and the proposed method are 616 and 878 s, respectively.

Finally, the EHD analysis of a lubricated cylindrical joint with rotating journal is presented. The length of the cylindrical joint is equal to 66 mm. The journal rotates around its axis A_jW_j at a constant angular speed of 3000 rpm. The dynamic lubricant viscosity is equal to 9 mPa s. The rigid journal is modeled by using the NCF, while the flexible bearing is modeled by the twenty-node hexahedral element of ANCF. The nodes on the outer bearing surface are assumed to be fixed in the space. The material density and the thickness of the bearing are set to be 7,800 kg/m^3 and 20 mm, respectively. As a comparison, the systems with and without journal misalignment are studied.

At first, the journal axis A_jW_j is assumed to be parallel with the bearing axis A_bW_b, that is, the rigid rotating journal is not misaligned being $e_1 = e_2 = 0.024$ mm. The clearance is equal to 0.03 mm. The Young's modulus of the bearing material is set to be 2.1×10^{12} Pa so that the results can be compared to those obtained by Sun and Gui [9], who considered a case of rigid bearing. Figure 10 shows the lubricant pressure distributions for this journal bearing system. As expected, Fig. 10b shows that if the journal is not misaligned, the lubricant pressure exhibits a symmetrical

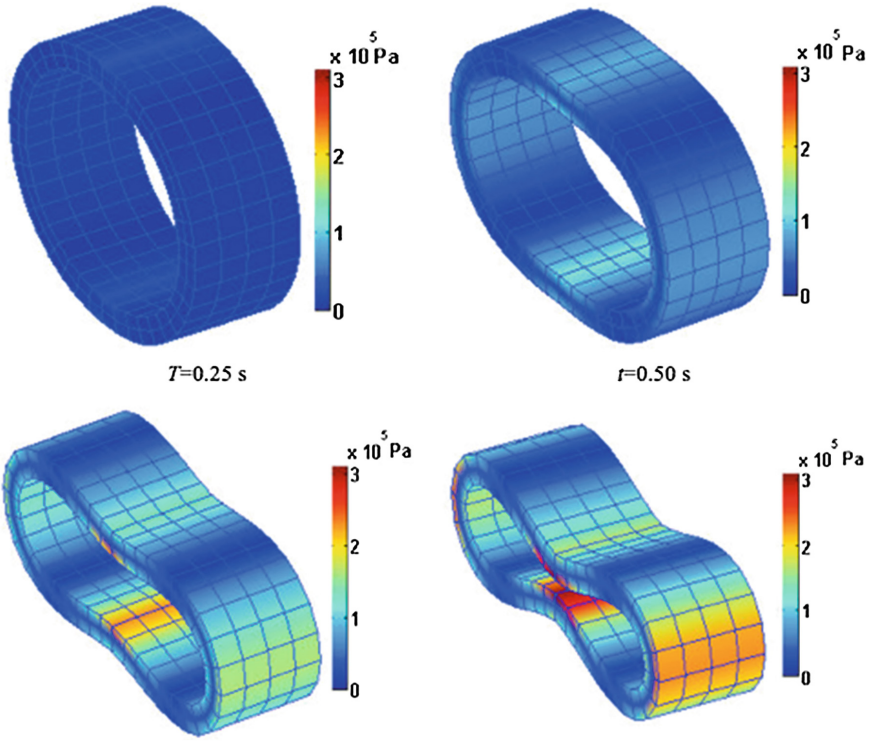

Fig. 8 von Mises stress contour of a *hollow cylinder* obtained using FEM of ANCF

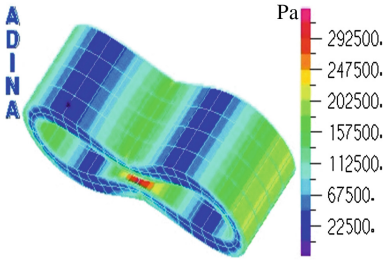

Fig. 9 The von Mises stress contour of a *hollow cylinder* obtained using ADINA (t = 1.00 s)

distribution about the plane ξ-C_j-η. Here, C_j is the mass center of the rigid journal. Figure 11 shows a scaled view of the deformation of the inner bearing surface. The figure indicates that for the system with a rotating journal without misalignment, the distribution of the deformation of the inner bearing surface also exhibits a symmetrical distribution about the plane ξ-C_j-η, which is consistent with the lubricant pressure distribution shown in Fig. 10b.

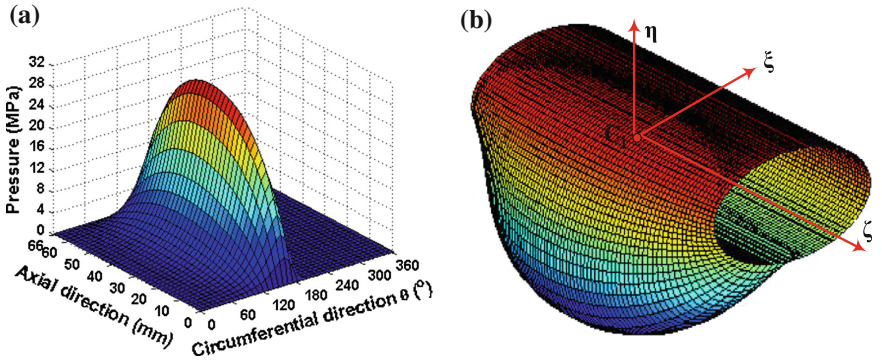

Fig. 10 Lubricant pressure distributions of a journal without misalignment ($E = 2.1 \times 10^{12}$ Pa). **a** pressure vs journal directions, **b** a 3D view

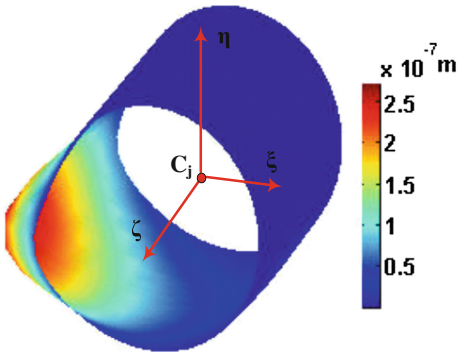

Fig. 11 Zoom view of the elastic deformation of inner bearing surface ($E = 2.1 \times 10^{12}$ Pa)

5 Conclusion

In the present study, a general and comprehensive methodology is proposed to integrate the EHD model of lubricated cylindrical joints into the flexible multibody system formulation. The EHD behavior of the lubricated cylindrical joints in flexible multibody system is studied by using the ACB method such that the flexible bearing is modeled via the twenty-node hexahedral elements of ANCF, while the rigid journal in the cylindrical joint is described via NCF. The lubricant pressure is evaluated by solving the Reynolds' equation via the finite difference method. The elastic forces and their Jacobian of ANCF finite elements are deducted through the definition of the Piola-Kirchhoff stress tensor of the first type in continuum mechanics. The numerical examples show that the bearing flexibility affects the system responses in a significant manner, since the flexible bearing will extend the lubricant distribution space, and then reduce the lubricant pressure. The methodology proposed in this study can be easily extended to studying the coupling dynamics of the lubricated rotor system with the bearing flexibility taken into account.

References

1. Attia HM, Bouziz S, Maatar M, Fakhfakh T, Haddar M (2010) Hydrodynamic and elastohydrodynamic studies of a cylindrical journal bearing. J Hydrodyn 22(2):155−163
2. Bathe KJ (2010) ADINA system. ADINA R&D Inc.
3. Jalón JG, Bayo E (1994) Kinematic and dynamic simulation of multibody systems: the real-time challenge. Springer, New York
4. Kumar MS, Thyla PR, Anbarasu E (2010) Numerical analysis of hydrodynamic journal bearing under transient dynamic conditions. Mechanika 2(82):37−42
5. Liu HP, Xu H, Ellision PJ, Jin ZM (2010) Application of computational fluid dynamics and fluid-structure interaction method to the lubrication study of a rotor bearing system. Tribol Lett 38(3):325−336
6. Nikravesh PE (1988) Computer aided analysis of mechanical systems. Prentice-Hall, New Jersey
7. Pinkus O, Sternlicht SA (1961) Theory of hydrodynamic lubrication. McGraw-Hill, New York
8. Shabana AA, Yakoub RY (2001) Three-dimensional absolute nodal coordinate formulation for beam elements: theory. J Mech Des 123:606−613
9. Sun J, Gui CL (2004) Hydrodynamic lubrication analysis of journal bearing considering misalignment caused by shaft deformation. Tribol Int 37:841−848
10. Tian Q, Liu C, Machado M, Flores P (2011) A new model for dry and lubricated cylindrical joints with clearance in spatial flexible multibody systems. Nonlinear Dyn 64:25−67